Gap solitons in fiber bragg gratings having polynomial law of nonlinear refractive index and cubic–quartic dispersive reflectivity by lie symmetry.

symmetry

MDPI

Article

Gap Solitons in Fiber Bragg Gratings Having Polynomial Law of Nonlinear Refractive Index and Cubic–Quartic Dispersive Reflectivity by Lie Symmetry

Sandeep Malik [1], Sachin Kumar [1], Anjan Biswas [2,3,4,5,6], Yakup Yıldırım [7], Luminita Moraru [8,*], Simona Moldovanu [9], Catalina Iticescu [8], Seithuti P. Moshokoa [10], Dorin Bibicu [11] and Abdulaziz Alotaibi [12]

1 Department of Mathematics and Statistics, Central University of Punjab, Bathinda 151401, Punjab, India
2 Department of Mathematics and Physics, Grambling State University, Grambling, LA 71245, USA
3 Mathematical Modeling and Applied Computation (MMAC) Research Group, Department of Mathematics, King Abdulaziz University, Jeddah 21589, Saudi Arabia
4 Department of Applied Mathematics, National Research Nuclear University, 31 Kashirskoe Hwy, Moscow 115409, Russia
5 Department of Applied Sciences, Cross-Border Faculty of Humanities, Economics and Engineering, Dunarea de Jos University of Galati, 111 Domneasca Street, 800201 Galati, Romania
6 Department of Mathematics and Applied Mathematics, Sefako Makgatho Health Sciences University, Medunsa 0204, South Africa
7 Department of Computer Engineering, Biruni University, 34010 Istanbul, Turkey
8 Department of Chemistry, Physics and Environment, Faculty of Sciences and Environment, Dunarea de Jos University of Galati, 47 Domneasca Street, 800008 Galati, Romania
9 Department of Computer Science and Information Technology, Faculty of Automation, Computers, Electrical Engineering and Electronics, Dunarea de Jos University of Galati, 47 Domneasca Street, 800008 Galati, Romania
10 Department of Mathematics and Statistics, Tshwane University of Technology, Pretoria 0008, South Africa
11 Department of Business Administration, Faculty of Economics and Business Administration, Dunarea de Jos University of Galati, 59-61 Nicolae Balcescu Street, 800001 Galati, Romania
12 Department of Industrial Engineering, University of Tabuk, Tabuk 45512, Saudi Arabia
* Correspondence: luminita.moraru@ugal.ro

Abstract: The current paper recovers cubic–quartic optical solitons in fiber Bragg gratings having polynomial law of nonlinear refractive index structures. Lie symmetry analysis is carried out, starting with the basic analysis. Then, it is followed through with improved Kudryashov and generalized Arnous schemes. The parameter constraints are also identified for the existence of such solitons. Numerical surface plots support the adopted applied analysis.

Keywords: polynomial; Lie symmetry; solitons; Kudryashov; Arnous

Citation: Malik, S.; Kumar, S.; Biswas, A.; Yıldırım, Y.; Moraru, L.; Moldovanu, S.; Iticescu, C.; Moshokoa, S.P.; Bibicu, D.; Alotaib, A. Gap Solitons in Fiber Bragg Gratings Having Polynomial Law of Nonlinear Refractive Index and Cubic–Quartic Dispersive Reflectivity by Lie Symmetry. *Symmetry* **2023**, *15*, 963. https://doi.org/10.3390/sym15050963

Academic Editors: Javid Atai and Sergei D. Odintsov

Received: 7 February 2023
Revised: 4 April 2023
Accepted: 21 April 2023
Published: 23 April 2023

1. Introduction

The concept of cubic–quartic (CQ) solitons emerged about half a decade ago when it was realized that soliton sustainability becomes questionable with catastrophic consequences when chromatic dispersion (CD) tends to become depleted [1–5]. Therefore, third-order dispersion (3OD) and fourth-order dispersion (4OD) effects are included to replenish the low count of CD. Thus, CQ solitons were conceived [6–10]. Aside from this measure to counter low counts of CD, another approach is from an engineering marvel that introduces a grating structure in the internal walls of the fiber core, known as Bragg gratings after the engineer who first proposed this structure [11–15]. This grating structure also produces dispersive reflectivity, compensating for low dispersive effects. Thus, the two approaches would collectively ensure the safe transmission of solitons across intercontinental distances without any adverse effect.

The current paper models such a physical situation in fiber Bragg gratings with CQ dispersive effects. The source of self–phase modulation (SPM) comes from the polynomial

law of nonlinear refractive index [3,4,11,14]. The model is therefore the coupled nonlinear Schrodinger's equation (NLSE) that is addressed in the paper. A Lie symmetry analysis first reduces the corresponding partial differential equations (PDEs) into ordinary differential equations (ODEs) that are subsequently addressed using the improved Kudryashov scheme and the generalized Arnous method. This gave way to retrieving singular and bright optoelectronic wave fields with the model presented in the paper. The supporting surface plots for the bright solitons are presented. The details are addressed after a succinct picture of the model.

Governing Equations

Periodic structures called Bragg gratings can be created by etching into an optical fiber [16–20]. Bragg gratings have a unique property: they reflect light of a specific wavelength while allowing light of other wavelengths to pass through [21–25]. This is possible because the grating's period and the fiber core's refractive index determine the wavelength of the reflected light. To address the problem of limited bandwidth in fiber optic communication systems due to increasing data demands, Bragg gratings can serve as a solution by increasing the capacity of the optical fiber [26–30]. This capacity issue occurs when the available bandwidth of a system becomes depleted, and is often referred to as CD running low. By incorporating Bragg gratings, the system can be optimized to accommodate higher data rates while maintaining the integrity of the signal [31–35]. Wavelength division multiplexing (WDM) is a technique that can be used to increase the capacity of an optical fiber by transmitting multiple signals simultaneously over different wavelengths in the same fiber. To implement WDM, Bragg gratings can be used to create filters that are specific to certain wavelengths [36–40]. These filters can separate the different signals, allowing multiple channels to operate at different wavelengths within the same fiber. By using Bragg gratings in this way, the fiber's capacity can be significantly increased, enabling it to accommodate a greater amount of data traffic [41–46]. Bragg gratings have another important application in the field of optical amplifiers, which are used to increase the strength of the signal in the fiber. By using Bragg gratings in conjunction with erbium-doped fiber amplifiers (EDFAs), it is possible to achieve wavelength-specific amplification. This feature enables multiple signals at different wavelengths to be amplified simultaneously, resulting in a significant increase in the overall capacity of systems. By implementing Bragg gratings in optical amplifiers, it is possible to achieve more efficient and effective signal amplification, making it possible to transmit data over longer distances with fewer errors. In the field of fiber optic communication, Bragg gratings have emerged as a versatile and powerful tool for increasing the capacity of the system. By enabling wavelength division multiplexing and providing wavelength-specific amplification in optical amplifiers, Bragg gratings offer a reliable and effective means of boosting the performance of fiber optic communication systems. With their ability to accommodate multiple signals at different wavelengths and amplify these signals with precision, Bragg gratings are an essential technology for meeting the growing demands of modern data transmission.

Bragg gratings have a multitude of applications in the context of chromatic dispersion (CD) running low in optical communication systems. Chromatic dispersion is a phenomenon that can cause signal distortion as different wavelengths of light travel at varying speeds through the fiber. Bragg gratings can be utilized to mitigate the effects of CD by creating wavelength-specific filters that compensate for the differences in propagation velocities. This approach can help to improve the quality and reliability of optical communication systems, particularly over long distances, by minimizing signal distortion and maintaining the integrity of the transmitted data. In addition to the applications mentioned earlier, Bragg gratings have proven to be a powerful tool for addressing CD-related issues in fiber optic communication. Furthermore, Bragg gratings have several other important applications and physical significance related to chromatic dispersion (CD) running low. These applications include the following: one key application of Bragg gratings in the context of chromatic dispersion (CD) running low is the compensation of CD-induced

signal distortion. Bragg gratings can be designed to induce a precise phase shift in reflected light, which can offset the phase shift induced by CD. By doing so, the distortion of the optical signal can be reduced or eliminated, thereby improving the quality and reliability of data transmission. This capability is particularly important in high-capacity optical communication systems, where the effects of CD can become a significant limiting factor in the performance of the system. Bragg gratings are a versatile and essential tool in optical fiber communication engineering. They can be used to address a range of issues related to chromatic dispersion, including compensating for dispersion slope and mitigating the effects of CD-induced signal distortion. Additionally, Bragg gratings can provide sensing capabilities for monitoring a variety of environmental parameters, making them an important technology for a range of applications. With their ability to enhance the performance and reliability of fiber optic communication systems, Bragg gratings are a key component in the design and implementation of cutting-edge optical communication networks.

The mathematical model that governs CQ solitons in fiber Bragg gratings with the polynomial form of SPM [47] is structured as:

$$\begin{aligned} &iq_t + ia_1 r_{xxx} + b_1 r_{xxxx} + \left(c_1|q|^2 + d_1|r|^2\right)q + \left(\xi_1|q|^4 + \eta_1|q|^2|r|^2 + \zeta_1|r|^4\right)q \\ &+\left(l_1|q|^6 + m_1|q|^4|r|^2 + n_1|q|^2|r|^4 + p_1|r|^6\right)q + i\alpha_1 q_x + \beta_1 r = 0, \end{aligned} \tag{1}$$

and

$$\begin{aligned} &ir_t + ia_2 q_{xxx} + b_2 q_{xxxx} + \left(c_2|r|^2 + d_2|q|^2\right)r + \left(\xi_2|r|^4 + \eta_2|q|^2|r|^2 + \zeta_2|r|^4\right)r \\ &+\left(l_2|r|^6 + m_2|r|^4|q|^2 + n_2|r|^2|q|^4 + p_2|q|^6\right)r + i\alpha_2 r_x + \beta_2 q = 0. \end{aligned} \tag{2}$$

For $j = 1, 2$, β_j gives the detuning parameters, and α_j yields the intermodal dispersion. d_j comes from the cross–phase modulation (XPM) for cubic nonlinearity, while $q(x,t)$ and $r(x,t)$ are the wave profiles propagating forwards and backwards in sequence. Next, a_j and b_j indicate the coefficients of 3OD and 4OD reflectivity in sequence, while c_j stems from the SPM. The XPM coefficients are given by m_j, n_j and p_j, while the coefficients ξ_j are for the SPM. Furthermore, from septic nonlinearity, the SPM coefficients are l_j, while η_j and ζ_j arise from the XPM.

2. Lie Symmetry Analysis

The Norwegian mathematician Marius Sophus Lie (1842–1899) discovered the Lie group theory. According to Lie, the various approaches to solving differential equations precisely were simply various applications of a general approach to integration, known as the theory of transformation groups. Lie theory is the mathematical foundation for understanding the symmetry of differential equations. Lie's introduction of the theory was so insightful that it allowed mathematicians to come up with many different methods and techniques for solving differential equations. Differential equations using symmetry analysis are becoming increasingly common in mathematics and the physical sciences, due to their effectiveness in solving complex problems. Tanwar et al. studied the propagation of some nonlinear dispersive water waves, such as waves in an infinitely narrow channel [48], waves with nonuniform velocities [49], waves in two horizontal directions in shallow water [50], the long wave equation with a large wavelength [51], and undulating bores in shallow water [52], by using Lie symmetry analysis. Some recent and very useful books devoted to Lie symmetry analysis are [53–57].

Here, Lie group analysis is used to derive the symmetry reduction of the system (1) and (2). Let us start by defining $r(x,t)$ and $q(x,t)$ as follows:

$$r(x,t) = u_2(x,t) + \iota v_2(x,t), \tag{3}$$

and

$$q(x,t) = u_1(x,t) + \iota v_1(x,t), \tag{4}$$

which divide the system (1) and (2) into the following systems

$$\begin{aligned} 0 = &-v_{it} - a_i v_{jxxx} + b_i u_{jxxxx} + \left[c_i\left(u_i^2+v_i^2\right) + d_i\left(u_j^2+v_j^2\right)\right]u_i + \left[\xi_i\left(u_i^2+v_i^2\right)^2\right. \\ &+\eta_i\left(u_i^2+v_i^2\right)\left(u_j^2+v_j^2\right) + \zeta_i\left(u_j^2+v_j^2\right)^2\Big]u_i + \left[l_i\left(u_i^2+v_i^2\right)^3 + m_i\left(u_i^2+v_i^2\right)^2\right. \\ &\left.\left(u_j^2+v_j^2\right) + n_i\left(u_i^2+v_i^2\right)\left(u_j^2+v_j^2\right)^2 + p_i\left(u_j^2+v_j^2\right)^3\right]u_i - \alpha_i v_{ix} + \beta_i u_j, \end{aligned} \tag{5}$$

and

$$\begin{aligned} 0 = &\,u_{it} + a_i u_{jxxx} + b_i v_{jxxxx} + \left[c_i\left(u_i^2+v_i^2\right) + d_i\left(u_j^2+v_j^2\right)\right]v_i + \left[\xi_i\left(u_i^2+v_i^2\right)^2\right. \\ &+\eta_i\left(u_i^2+v_i^2\right)\left(u_j^2+v_j^2\right) + \zeta_i\left(u_j^2+v_j^2\right)^2\Big]v_i + \left[l_i\left(u_i^2+v_i^2\right)^3 + m_i\left(u_i^2+v_i^2\right)^2\right. \\ &\left.\left(u_j^2+v_j^2\right) + n_i\left(u_i^2+v_i^2\right)\left(u_j^2+v_j^2\right)^2 + p_i\left(u_j^2+v_j^2\right)^3\right]v_i + \alpha_i u_{ix} + \beta_i v_j, \end{aligned} \tag{6}$$

where $j = 3 - i$ and $i = 1, 2$. To derive symmetries for the system (5) and (6), the Lie group of point transformations is presented as below:

$$\begin{aligned} v_2^* &= v_2 + \epsilon\,\psi_2(x,t,u_1,u_2,v_1,v_2) + O(\epsilon^2), \\ v_1^* &= v_1 + \epsilon\,\psi_1(x,t,u_1,u_2,v_1,v_2) + O(\epsilon^2), \\ u_2^* &= u_2 + \epsilon\,\phi_2(x,t,u_1,u_2,v_1,v_2) + O(\epsilon^2), \\ u_1^* &= u_1 + \epsilon\,\phi_1(x,t,u_1,u_2,v_1,v_2) + O(\epsilon^2), \\ t^* &= t + \epsilon\,\tau(x,t,u_1,u_2,v_1,v_2) + O(\epsilon^2), \\ x^* &= x + \epsilon\,\xi(x,t,u_1,u_2,v_1,v_2) + O(\epsilon^2), \end{aligned} \tag{7}$$

where ϕ_2, τ, ϕ_1, ξ, ψ_2 and ψ_1 are infinitesimals that can be achieved by linearizing the invariance condition about $\epsilon = 0$. The vector field V connected to the Lie group of transformations (7) mentioned above is

$$V = \xi\frac{\partial}{\partial x} + \tau\frac{\partial}{\partial t} + \phi_1\frac{\partial}{\partial u_1} + \phi_2\frac{\partial}{\partial u_2} + \psi_1\frac{\partial}{\partial v_1} + \psi_2\frac{\partial}{\partial v_2}. \tag{8}$$

The system of invariance conditions is generated by applying the transformations (7) to the system (5) and (6). The values of the appropriate extended infinitesimals should then be substituted, and the coefficient of the various powers of the differentials of u_1, u_2, v_1, v_2 should be equalized to provide a system of determining equations. The following are the resultant infinitesimals that are acquired by resolving the system of determining equations:

$$\xi = C_2, \quad \tau = C_1, \quad \phi_1 = -C_3 v_1, \quad \phi_2 = -C_3 v_2, \quad \psi_1 = C_3 u_1, \quad \psi_2 = C_3 u_2, \tag{9}$$

where C_1, C_2 and C_3 are arbitrary constants. As a result, the infinitesimal generators derived from (9) are extracted as

$$V_1 = \frac{\partial}{\partial t}, \quad V_2 = \frac{\partial}{\partial x}, \quad V_3 = u_2\frac{\partial}{\partial v_2} + u_1\frac{\partial}{\partial v_1} - v_2\frac{\partial}{\partial u_2} - v_1\frac{\partial}{\partial u_1}. \tag{10}$$

The Lie algebra (10) comprises some additional Lie symmetry for the system (1) and (2). For example, if we consider system (1) and (2) with the non-zero b_i, c_i, d_i, and all other parameters vanish, then the Lie algebra (10) admits the additional Lie symmetry

$$V_4 = 4t\frac{\partial}{\partial t} + x\frac{\partial}{\partial x} - 2u_1\frac{\partial}{\partial u_1} - 2u_2\frac{\partial}{\partial u_2} - 2v_1\frac{\partial}{\partial v_1} - 2v_2\frac{\partial}{\partial v_2}. \tag{11}$$

Consider the system (1) and (2) with the non-zero $b_i, \xi_i, \eta_i, \zeta_i$; all other parameters vanish. In this case, the system (1) and (2) admits the additional Lie symmetry as

$$V_4 = 4t\frac{\partial}{\partial t} + x\frac{\partial}{\partial x} - u_1\frac{\partial}{\partial u_1} - u_2\frac{\partial}{\partial u_2} - v_1\frac{\partial}{\partial v_1} - v_2\frac{\partial}{\partial v_2}. \tag{12}$$

Consider the system (1) and (2) with the non-zero a_i, c_i, d_i; all other parameters vanish. In this case, the system (1) and (2) admits the additional Lie symmetry as

$$V_4 = 3t\frac{\partial}{\partial t} + x\frac{\partial}{\partial x} - \frac{3u_1}{2}\frac{\partial}{\partial u_1} - \frac{3u_2}{2}\frac{\partial}{\partial u_2} - \frac{3v_1}{2}\frac{\partial}{\partial v_1} - \frac{3v_2}{2}\frac{\partial}{\partial v_2}. \tag{13}$$

Consider the system (1) and (2) with the non-zero $a_i, \xi_i, \eta_i, \zeta_i$; all other parameters vanish. In this case, the system (1) and (2) admits the additional Lie symmetry as

$$V_4 = 3t\frac{\partial}{\partial t} + x\frac{\partial}{\partial x} - \frac{3u_1}{4}\frac{\partial}{\partial u_1} - \frac{3u_2}{4}\frac{\partial}{\partial u_2} - \frac{3v_1}{4}\frac{\partial}{\partial v_1} - \frac{3v_2}{4}\frac{\partial}{\partial v_2}. \tag{14}$$

Symmetry Reduction

In this subsection, we reduce the system (1) and (2) into coupled ordinary differential equations by considering the Lie algebra (10)–(14).

Case 1: For the vector field

$$V_3 + \lambda V_2 + \mu V_1 = u_2\frac{\partial}{\partial v_2} + u_1\frac{\partial}{\partial v_1} - v_2\frac{\partial}{\partial u_2} - v_1\frac{\partial}{\partial u_1} + \mu\frac{\partial}{\partial t} + \lambda\frac{\partial}{\partial x}, \tag{15}$$

the corresponding similarity variables are recovered as

$$\begin{aligned} v_2(x,t) &= P_2(\sigma)\sin(Q_2(\sigma)),\\ u_2(x,t) &= P_2(\sigma)\cos(Q_2(\sigma)),\\ v_1(x,t) &= P_1(\sigma)\sin(Q_1(\sigma)),\\ u_1(x,t) &= P_1(\sigma)\cos(Q_1(\sigma)),\\ \sigma &= \mu x - \lambda t, \end{aligned} \tag{16}$$

where λ and μ are non-zero constants, while P_1 and P_2 are new dependent variables. By utilizing (16), along with the relation

$$Q_1(\sigma) = Q_2(\sigma) = Q(\sigma), \tag{17}$$

the system (5) and (6) reduces to

$$\begin{aligned} 0 = {} & \lambda Q' P_i - a_i\mu^3\left[-(Q')^3P_j + 3Q'P_j'' + 3Q''P_j' + Q'''P_j\right] + b_i\mu^4\left[(Q')^4P_j - 6(Q')^2P_j''\right.\\ & \left.-12Q'Q''P_j' - 4Q'Q'''P_j - 3(Q'')^2P_j + P_j''''\right] + \left[c_iP_i^2 + d_iP_j^2\right]P_i + \left[\xi_iP_i^4 + \eta_iP_i^2P_j^2\right.\\ & \left.+\zeta_iP_j^2\right]P_i + \left[l_iP_i^6 + m_iP_i^4P_j^2 + n_iP_i^2P_j^4 + p_iP_j^6\right]P_i - \alpha_i\mu Q'P_i + \beta_iP_j, \end{aligned} \tag{18}$$

and

$$0 = -\lambda P_i' + a_i\mu^3\left[-3(Q')^2P_j' - 3Q'Q''P_j + P_j'''\right] + b_i\mu^4\left[-4(Q')^3P_j' - 6(Q')^2Q''P_j + 4Q'P_j''' + 6Q''P_j'' + 4Q'''P_j' + Q''''P_j\right] + \alpha_i\mu P_i', \tag{19}$$

where $j = 3 - i$ and $i = 1, 2$. Now, from (19), comparing the coefficient of P_j''' equal to zero, gives

$$Q(\sigma) = -\frac{a_i}{4\mu b_i}\sigma + k_1, \tag{20}$$

where k_1 is the constant of integration. Next, let us consider

$$\begin{aligned}
&P_2 = \rho P_1,\\
&\lambda = \mu\alpha_1 - \frac{\mu\rho a_1^3}{8b_1^2} = \mu\alpha_2 - \frac{\mu\rho a_2^3}{8b_2^2},\\
&(\rho^6 p_1 + \rho^4 n_1 + \rho^2 m_1 + l_1) = \rho(\rho^6 l_2 + \rho^4 m_2 + \rho^2 n_2 + p_2),\\
&(\rho^4\zeta_1 + \rho^2\eta_1 + \xi_1) = \rho(\rho^4\xi_2 + \rho^2\eta_2 + \zeta_2),\\
&(\rho^2 d_1 + c_1) = (\rho^2 c_2 + d_2),\\
&\left(\beta_1 - \frac{3a_1^4}{256b_1^3}\right)\rho - \frac{a_1}{4\mu b_1}(\lambda - \mu\alpha_1) = -\frac{a_2\rho}{4\mu b_2}(\lambda - \mu\alpha_2) + \beta_2 - \frac{3a_2^4}{256b_2^3},\\
&\frac{a_1^2\rho}{b_1} = \frac{a_2^2}{b_2},\\
&b_1\rho = b_2.
\end{aligned} \tag{21}$$

Utilizing (20), along with the restrictions of (21), the system of Equations (18) and (19) leads to

$$S_1P_1'''' + S_2P_1'' + S_3P_1^7 + S_4P_1^5 + S_5P_1^3 + S_6P_1 = 0, \tag{22}$$

where

$$\begin{aligned}
S_1 &= \rho b_1\mu^4,\\
S_2 &= \frac{3\rho\mu^2 a_1^2}{8b_1},\\
S_3 &= (\rho^6 p_1 + \rho^4 n_1 + \rho^2 m_1 + l_1),\\
S_4 &= (\rho^4\zeta_1 + \rho^2\eta_1 + \xi_1),\\
S_5 &= (\rho^2 d_1 + c_1),\\
S_6 &= \left(\beta_1 - \frac{3a_1^4}{256b_1^3}\right)\rho - \frac{a_1}{4\mu b_1}(\lambda - \mu\alpha_1).
\end{aligned} \tag{23}$$

Now, by setting

$$P_1(\sigma) = U(\sigma)^{\frac{2}{3}}, \tag{24}$$

Equation (22) changes to

$$81S_3U^8 + 81S_4U^{\frac{20}{3}} + 81S_5U^{\frac{16}{3}} + 81S_6U^4 + 54[S_1U'''' + S_2U'']U^3 - 18\Big[S_2(U')^2 + 4S_1U'U''' + 3S_1(U'')^2\Big]U^2 + 144S_1U(U')^2U'' - 56S_1(U')^4 = 0. \tag{25}$$

For integrability aspects, one can set

$$S_4 = S_5 = 0. \tag{26}$$

So, Equation (25) becomes

$$81S_3U^8 + 81S_6U^4 + 54[S_1U'''' + S_2U'']U^3 - 18\Big[S_2(U')^2 + 4S_1U'U''' + 3S_1(U'')^2\Big]U^2 + 144S_1U(U')^2U'' - 56S_1(U')^4 = 0. \tag{27}$$

Case 2: For the vector field given by (11)

$$V_4 = 4t\frac{\partial}{\partial t} + x\frac{\partial}{\partial x} - 2u_1\frac{\partial}{\partial u_1} - 2u_2\frac{\partial}{\partial u_2} - 2v_1\frac{\partial}{\partial v_1} - 2v_2\frac{\partial}{\partial v_2}, \tag{28}$$

the corresponding similarity variables are recovered as

$$v_2(x,t) = \frac{Q_2(\sigma)}{\sqrt{t}}, \quad u_2(x,t) = \frac{P_2(\sigma)}{\sqrt{t}}, \quad v_1(x,t) = \frac{Q_1(\sigma)}{\sqrt{t}}, \quad u_1(x,t) = \frac{P_1(\sigma)}{\sqrt{t}}, \quad \sigma = \frac{x^4}{t}, \tag{29}$$

where P_i and Q_i are new dependent variables. By utilizing (29), the system (5) and (6) reduces to

$$0 = c_iP_i^3 + \Big(d_iQ_j^2 + c_iQ_i^2 + d_iP_j^2\Big)P_i + \tfrac{1}{2}Q_i + 256\sigma^3b_iP_j'''' + 1152\sigma^2b_iP_j''' + 816\sigma b_iP_j'' + \sigma Q_i' + 24b_iP_j', \tag{30}$$

and

$$0 = c_iP_i^2Q_i - \tfrac{1}{2}P_i + c_iQ_i^3 + d_i\Big(P_j^2 + Q_j^2\Big)Q_i + 256\sigma^3b_iQ_j'''' + 1152\sigma^2b_iQ_j''' + 816\sigma b_iQ_j'' - \sigma P_i' + 24b_iQ_j', \tag{31}$$

where $j = 3 - i$ and $i = 1, 2$.

Case 3: For the vector field given by (12)

$$V_4 = 4t\frac{\partial}{\partial t} + x\frac{\partial}{\partial x} - u_1\frac{\partial}{\partial u_1} - u_2\frac{\partial}{\partial u_2} - v_1\frac{\partial}{\partial v_1} - v_2\frac{\partial}{\partial v_2}, \tag{32}$$

the corresponding similarity variables are recovered as

$$v_2(x,t) = \frac{Q_2(\sigma)}{x}, \quad u_2(x,t) = \frac{P_2(\sigma)}{x}, \quad v_1(x,t) = \frac{Q_1(\sigma)}{x}, \quad u_1(x,t) = \frac{P_1(\sigma)}{x}, \quad \sigma = \frac{x^4}{t}, \tag{33}$$

where P_i and Q_i are new dependent variables. By utilizing (33), the system (5) and (6) reduces to

$$0 = \xi_iP_i^5 + \Big(2\xi_iQ_i^2 + \eta_i\Big(Q_j^2 + P_j^2\Big)\Big)P_i^3 + \Big(\xi_iQ_i^4 + \eta_i\Big(Q_j^2 + P_j^2\Big)Q_i + \zeta_i\Big(Q_j^2 + P_j^2\Big)^2\Big)P_i + 24b_iP_j + 432b_i\sigma^2P_j'' + 896b_i\sigma^3P_j''' + 256b_i\sigma^4P_j'''' + \sigma^2Q_i' - 24b_i\sigma P_j', \tag{34}$$

and

$$0=\eta_i\left(Q_j^2+P_j^2\right)Q_i^3+\xi_iQ_i^5+\left(2\xi_iQ_i^2+\eta_i\left(Q_j^2+P_j^2\right)\right)Q_iP_i^2+\zeta_i\left(Q_j^2+P_j^2\right)^2Q_i+24b_iQ_j \\ +\xi_iP_i^4Q_i+256b_i\sigma^4Q_j''''-24b_i\sigma Q_j'-\sigma^2P_i'+896b_i\sigma^3Q_j'''+432b_i\sigma^2Q_j'', \tag{35}$$

where $j=3-i$ and $i=1,2$.

Case 4: For the vector field given by (13)

$$V_4=3t\frac{\partial}{\partial t}+x\frac{\partial}{\partial x}-\frac{3u_1}{2}\frac{\partial}{\partial u_1}-\frac{3u_2}{2}\frac{\partial}{\partial u_2}-\frac{3v_1}{2}\frac{\partial}{\partial v_1}-\frac{3v_2}{2}\frac{\partial}{\partial v_2}, \tag{36}$$

the corresponding similarity variables are recovered as

$$v_2(x,t)=\frac{Q_2(\sigma)}{\sqrt{t}},\quad u_2(x,t)=\frac{P_2(\sigma)}{\sqrt{t}},\quad v_1(x,t)=\frac{Q_1(\sigma)}{\sqrt{t}},\quad u_1(x,t)=\frac{P_1(\sigma)}{\sqrt{t}},\quad \sigma=\frac{x^3}{t}, \tag{37}$$

where P_i and Q_i are new dependent variables. By utilizing (37), the system (5) and (6) reduces to

$$0=c_iP_i^3+\left(d_iQ_j^2+c_iQ_i^2+d_iP_j^2\right)P_i+\tfrac{1}{2}Q_i-54\sigma a_iQ_j''-27\sigma^2a_iQ_j'''+\sigma Q_i'-6a_iQ_j', \tag{38}$$

and

$$0=P_i^2Q_ic_i-\tfrac{P_i}{2}+Q_i^3c_i+\left(Q_j^2d_i+P_j^2d_i\right)Q_i+54\sigma a_iP_j''+27\sigma^2a_iP_j'''-\sigma P_i'+6a_iP_j', \tag{39}$$

where $j=3-i$ and $i=1,2$.

Case 5: For the vector field given by (14)

$$V_4=3t\frac{\partial}{\partial t}+x\frac{\partial}{\partial x}-\frac{3u_1}{4}\frac{\partial}{\partial u_1}-\frac{3u_2}{4}\frac{\partial}{\partial u_2}-\frac{3v_1}{4}\frac{\partial}{\partial v_1}-\frac{3v_2}{4}\frac{\partial}{\partial v_2}, \tag{40}$$

the corresponding similarity variables are recovered as

$$v_2(x,t)=\frac{Q_2(\sigma)}{\sqrt[4]{t}},\quad u_2(x,t)=\frac{P_2(\sigma)}{\sqrt[4]{t}},\quad v_1(x,t)=\frac{Q_1(\sigma)}{\sqrt[4]{t}},\quad u_1(x,t)=\frac{P_1(\sigma)}{\sqrt[4]{t}},\quad \sigma=\frac{x^3}{t}, \tag{41}$$

where P_i and Q_i are new dependent variables. By utilizing (41), the system (5) and (6) reduces to

$$0=\xi_iP_i^5+\left(2\xi_iQ_i^2+\eta_i\left(Q_j^2+P_j^2\right)\right)P_i^3+\left(\xi_iQ_i^4+\eta_i\left(Q_j^2+P_j^2\right)Q_i^2+\zeta_iQ_j^4+2\zeta_iP_j^2Q_j^2 \\ +\zeta_iP_j^4\right)P_i+\tfrac{1}{4}Q_i-54\sigma a_iQ_j''-27\sigma^2a_iQ_j'''+\sigma Q_i'-6a_iQ_j', \tag{42}$$

and

$$0=\xi_iQ_i^5-\tfrac{1}{4}P_i+\left(2\xi_iQ_i+\eta_i\left(Q_j^2+P_j^2\right)\right)Q_iP_i^2+\left(2\zeta_iP_j^2Q_j^2+\zeta_iP_j^4+\zeta_iQ_j^4\right)Q_i \\ +\xi_iP_i^4Q_i+\eta_i\left(Q_j^2+P_j^2\right)Q_i^3+27\sigma^2a_iP_j'''+54\sigma a_iP_j''+6a_iP_j''-\sigma P_i', \tag{43}$$

where $j=3-i$ and $i=1,2$.

It is difficult to express the exact solutions of coupled ordinary differential equations derived in the above cases (2)–(5), but one can express their solutions in the numerical forms.

3. Improved Kudryashov Method

Under the circumstances of the improved Kudryashov method [58], Equation (27) satisfies the explicit solution of the form

$$U(\sigma) = B_0 + B_1 R(\sigma), \tag{44}$$

where B_0 and B_1 are arbitrary constants, with $B_1 \neq 0$. In (44), the function $R(\sigma)$ fulfills the relation

$$R'(\sigma) = \delta\Big(\varrho R(\sigma)^3 - R(\sigma)\Big), \tag{45}$$

and possesses the solution

$$R(\sigma) = \frac{1}{\sqrt{\varrho + k\,\mathrm{e}^{2\delta\sigma}}}, \tag{46}$$

where k is a real constant. By inserting (44) into (27) and then utilizing (45), we receive a polynomial of $R(\sigma)$. Then, by gathering the coefficients of different powers of derived polynomials equal to zero, one secures a system of equations that permits the following results:

$$B_0 = 0, \quad B_1 = \pm\frac{4\delta}{3}\sqrt[4]{-\frac{22\varrho^2 S_1}{S_3}}, \quad S_2 = -\frac{68\delta^2 S_1}{9}, \quad S_6 = \frac{256\delta^4 S_1}{81}. \tag{47}$$

Therefore, the straddled soliton profiles are presented as below:

$$q(x,t) = \pm\left\{\frac{4\delta}{3}\sqrt[4]{-\frac{22\varrho^2 S_1}{S_3}}\left(\frac{1}{\sqrt{\varrho + k\,\mathrm{e}^{2\delta\left(\mu x - \left(\mu\alpha_1 - \frac{\mu\rho a_1^3}{8b_1^2}\right)t\right)}}}\right)\right\}^{\frac{2}{3}} \mathrm{e}^{i\left(-\frac{a_1}{4\mu b_1}\left(\mu x - \left(\mu\alpha_1 - \frac{\mu\rho a_1^3}{8b_1^2}\right)t\right) + k_1\right)}, \tag{48}$$

and

$$r(x,t) = \pm\rho\left\{\frac{4\delta}{3}\sqrt[4]{-\frac{22\varrho^2 S_1}{S_3}}\left(\frac{1}{\sqrt{\varrho + k\,\mathrm{e}^{2\delta\left(\mu x - \left(\mu\alpha_1 - \frac{\mu\rho a_1^3}{8b_1^2}\right)t\right)}}}\right)\right\}^{\frac{2}{3}} \mathrm{e}^{i\left(-\frac{a_1}{4\mu b_1}\left(\mu x - \left(\mu\alpha_1 - \frac{\mu\rho a_1^3}{8b_1^2}\right)t\right) + k_1\right)}, \tag{49}$$

with constraint $S_1 S_3 < 0$.

4. Generalized Arnous Method

In this section, we extract the optical soliton solutions of the system (1) and (2) by using the generalized Arnous scheme [59] on Equation (27). According to this method, Equation (27) holds the solution

$$P(\sigma) = \varrho_0 + \frac{\varrho_1 + \nu_1\Phi'(\sigma)}{\Phi(\sigma)}, \tag{50}$$

where ϱ_0, ϱ_1 and ν_1 are arbitrary constants. Here $\Phi(\sigma)$ satisfies the following relation

$$\big[\Phi'(\sigma)\big]^2 = \Big[\Phi(\sigma)^2 - \chi\Big]\ln(A)^2, \tag{51}$$

with

$$\Phi^{(n)}(\sigma) = \begin{cases} \Phi'(\sigma)\ln(A)^{n-1}, & n \text{ is odd}, \\ \Phi(\sigma)\ln(A)^n, & n \text{ is even}, \end{cases} \qquad n \geq 2 \tag{52}$$

where $A > 0$ and $A \neq 1$. Equation (51) admits a solution as shown below:

$$\Phi(\sigma) = \frac{\chi}{4k\ln(A)A^{\sigma}} + k\ln(A)A^{\sigma}, \tag{53}$$

where χ and k are arbitrary parameters.

By inserting (50) along with (51) into Equation (22), we receive a polynomial of $\frac{1}{\Phi(\sigma)}\left(\frac{\Phi'(\sigma)}{\Phi(\sigma)}\right)$. Then, by gathering the coefficients of different powers of derived polynomial equal to zero, one obtains a system of equations that admits the following results:

$$\varrho_0 = 0, \quad \nu_1 = 0, \quad \varrho_1 = \pm\frac{2\ln(A)}{3}\sqrt[4]{-\frac{55\chi^2 S_1}{S_3}}, \quad S_2 = -\frac{68\ln(A)^2 S_1}{9}, \quad S_6 = \frac{256\ln(A)^4 S_1}{81}. \tag{54}$$

Therefore, we reveal the straddled soliton profiles

$$q(x,t) = \pm\left\{\frac{2\ln(A)}{3}\sqrt[4]{-\frac{55\chi^2 S_1}{S_3}}\left(\frac{4k\ln(A)A^{\mu x-\left(\mu\alpha_1-\frac{\mu\rho a_1^3}{8b_1^2}\right)t}}{4k^2\ln(A)^2A^{2\mu x-2\left(\mu\alpha_1-\frac{\mu\rho a_1^3}{8b_1^2}\right)t}+\chi}\right)\right\}^{\frac{2}{3}} e^{i\left(-\frac{a_1}{4\mu b_1}\left(\mu x-\left(\mu\alpha_1-\frac{\mu\rho a_1^3}{8b_1^2}\right)t\right)+k_1\right)}, \tag{55}$$

and

$$r(x,t) = \pm\rho\left\{\frac{2\ln(A)}{3}\sqrt[4]{-\frac{55\chi^2 S_1}{S_3}}\left(\frac{4k\ln(A)A^{\mu x-\left(\mu\alpha_1-\frac{\mu\rho a_1^3}{8b_1^2}\right)t}}{4k^2\ln(A)^2A^{2\mu x-2\left(\mu\alpha_1-\frac{\mu\rho a_1^3}{8b_1^2}\right)t}+\chi}\right)\right\}^{\frac{2}{3}} e^{i\left(-\frac{a_1}{4\mu b_1}\left(\mu x-\left(\mu\alpha_1-\frac{\mu\rho a_1^3}{8b_1^2}\right)t\right)+k_1\right)}, \tag{56}$$

with constraint $S_1S_3 < 0$.

If we consider $\chi = 4k^2\log(A)^2$ in solutions (55) and (56), then we recover the bright optoelectronic wave fields

$$q(x,t) = \pm\left\{\frac{1}{3k}\sqrt[4]{-\frac{55\chi^2 S_1}{S_3}}\,\mathrm{sech}\left[\left(\mu x-\left(\mu\alpha_1-\frac{\mu\rho a_1^3}{8b_1^2}\right)t\right)\ln A\right]\right\}^{\frac{2}{3}} e^{i\left(-\frac{a_1}{4\mu b_1}\left(\mu x-\left(\mu\alpha_1-\frac{\mu\rho a_1^3}{8b_1^2}\right)t\right)+k_1\right)}, \tag{57}$$

and

$$r(x,t) = \pm\rho\left\{\frac{1}{3k}\sqrt[4]{-\frac{55\chi^2 S_1}{S_3}}\,\mathrm{sech}\left[\left(\mu x-\left(\mu\alpha_1-\frac{\mu\rho a_1^3}{8b_1^2}\right)t\right)\ln A\right]\right\}^{\frac{2}{3}} e^{i\left(-\frac{a_1}{4\mu b_1}\left(\mu x-\left(\mu\alpha_1-\frac{\mu\rho a_1^3}{8b_1^2}\right)t\right)+k_1\right)}, \tag{58}$$

while, if we consider $\chi = -4k^2\log(A)^2$ in solutions (55) and (56), then we recover the singular soliton profiles

$$q(x,t) = \pm\left\{\frac{1}{3k}\sqrt[4]{-\frac{55\chi^2 S_1}{S_3}}\,\mathrm{csch}\left[\left(\mu x-\left(\mu\alpha_1-\frac{\mu\rho a_1^3}{8b_1^2}\right)t\right)\ln A\right]\right\}^{\frac{2}{3}} e^{i\left(-\frac{a_1}{4\mu b_1}\left(\mu x-\left(\mu\alpha_1-\frac{\mu\rho a_1^3}{8b_1^2}\right)t\right)+k_1\right)}, \tag{59}$$

and

$$r(x,t) = \pm\rho\left\{\frac{1}{3k}\sqrt[4]{-\frac{55\chi^2 S_1}{S_3}}\,\mathrm{csch}\left[\left(\mu x-\left(\mu\alpha_1-\frac{\mu\rho a_1^3}{8b_1^2}\right)t\right)\ln A\right]\right\}^{\frac{2}{3}} e^{i\left(-\frac{a_1}{4\mu b_1}\left(\mu x-\left(\mu\alpha_1-\frac{\mu\rho a_1^3}{8b_1^2}\right)t\right)+k_1\right)}. \tag{60}$$

The surface plots of solitons (57) and (58) are depicted in Figure 1. The parameter values chosen are: $k = 1$, $\rho = 2$, $\mu = 1$, $p_1 = 1$, $n_1 = 1$, $m_1 = 1$, $l_1 = 1$, $\alpha_1 = 1$, $a_1 = 1$, $b_1 =$-1 and $A = e$. The surface plot of a bright soliton is a smooth, bell-shaped curve that remains relatively constant over time and space. The curve is localized in space and time, and its height corresponds to the amplitude of the soliton, while the x-coordinate represents

the spatial dimension, and the t-coordinate represents time. Bright solitons are known for their ability to maintain their shape and amplitude over long distances, due to a balance between dispersion and nonlinearity. This stability means that the surface plot of a bright soliton shows only minor fluctuations or deformations, which reflects the regular and predictable behavior of the soliton. The symmetrical nature of the surface plot indicates the stability and regularity of the soliton. These properties make bright solitons ideal for use in applications such as fiber optic communications or Bose-Einstein condensates in ultracold atomic gases, where stability and control are crucial. The surface plot of a bright soliton is a visual representation of a stable and localized wave phenomenon that can propagate over long distances without losing its shape or amplitude.

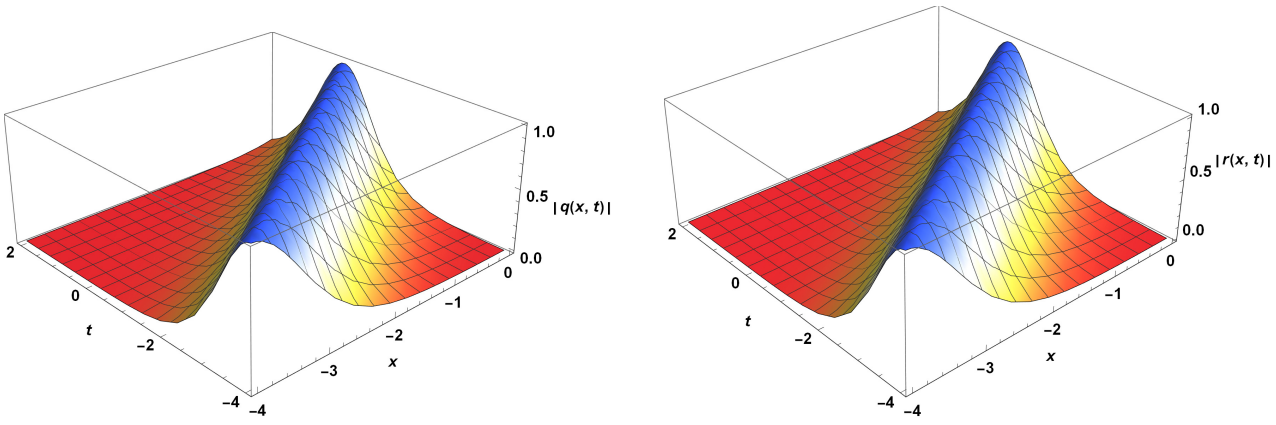

Figure 1. Profiles of bright solitons in fiber Bragg gratings.

5. Extended Tanh Technique

In this section, we derive optical soliton solutions of the system (1) and (2) by performing the extended tanh method [60] on Equation (27). The extended tanh scheme suggests the solution of Equation (27) as

$$U(\sigma) = A_0 + A_1 \tanh(m\xi) + A_{-1} \tanh^{-1}(m\xi) \tag{61}$$

where A_0, A_1 and A_{-1} are arbitrary constants. Plugging (61) into (27) yields a system of equations that satisfies the results:

$$A_0 = 0, \quad A_{-1} = -A_1, \quad m = 3\sqrt{-\frac{S_2}{272S_1}}, \quad S_3 = \pm\frac{55S_2^2}{4624S_1A_1^4}, \quad S_6 = \frac{16S_2^2}{289S_1}. \tag{62}$$

Hence, we achieve the singular optoelectronic wave fields

$$q(x,t) = \pm\frac{A_1}{4^{1/3}}\left\{\operatorname{csch}\left[2m_1\left(\mu x - \left(\mu\alpha_1 - \frac{\mu\rho a_1^3}{8b_1^2}\right)t\right)\right]\right\}^{\frac{2}{3}} \mathrm{e}^{i\left(-\frac{a_1}{4\mu b_1}\left(\mu x - \left(\mu\alpha_1 - \frac{\mu\rho a_1^3}{8b_1^2}\right)t\right) + k_1\right)}, \tag{63}$$

and

$$r(x,t) = \pm\frac{\rho A_1}{4^{1/3}}\left\{\operatorname{csch}\left[2m_1\left(\mu x - \left(\mu\alpha_1 - \frac{\mu\rho a_1^3}{8b_1^2}\right)t\right)\right]\right\}^{\frac{2}{3}} \mathrm{e}^{i\left(-\frac{a_1}{4\mu b_1}\left(\mu x - \left(\mu\alpha_1 - \frac{\mu\rho a_1^3}{8b_1^2}\right)t\right) + k_1\right)}, \tag{64}$$

with the constraint $S_1S_2 < 0$, and (62). So, in this case, we have singular solitons.

6. Conclusions

The current paper is about retrieving bright and singular CQ solitons in fiber Bragg gratings with the polynomial form of SPM. These soliton solutions are of great importance in the study of fiber Bragg gratings. The main approach is Lie symmetry analysis, which

reduced the PDEs to the corresponding ODEs that were addressed using a couple of newly proposed integration schemes, namely, the improved Kudryashov and generalized Arnous schemes. These new findings in the literature of solitons will lead to a number of new avenues to walk on. The conservation laws for the full-blown mathematical model are to be recovered, and this would naturally lead to quasistationary solitons and perturbation theory. In our analysis, it is not possible to come up with the conservation laws for Bragg gratings. This is due to the presence of dispersive reflectivity, as opposed to chromatic dispersion. Therefore, the multiplier approach fails to retrieve the conservation laws and fluxes. The failure attributed to the usage of the Lagrangian approach is similar.

The improved Kudryashov method and generalized Arnous method are both analytical techniques used to solve nonlinear partial differential equations (PDEs) that arise in various physical systems, including fiber Bragg gratings with polynomial law of nonlinear refractive index structures. The improved Kudryashov method is a powerful and efficient method for finding analytical solutions for nonlinear PDEs, particularly those with singularities. It has been used to find bright soliton solutions for various nonlinear systems, including fiber Bragg gratings. Bright solitons are characterized by a localized, finite amplitude that propagates without changing its shape. They are typically stable and can be used for applications such as signal processing and data transmission. On the other hand, the generalized Arnous method is an analytical method that is used to find singular soliton solutions for nonlinear PDEs. Singular solitons are characterized by a divergent amplitude at a particular point or points. They are less stable than bright solitons, but they can still be useful for certain applications in fields such as nonlinear optics and plasma physics. In our analysis, it seems that the improved Kudryashov method was able to find both bright and singular soliton solutions, while the generalized Arnous method was only able to find singular solitons. This suggests that the improved Kudryashov method may be a more powerful and versatile method for finding solutions to nonlinear PDEs in fiber Bragg gratings with polynomial law of nonlinear refractive index structures. However, the choice of method should depend on the specific requirements of the analysis and the properties of the solutions.

Author Contributions: Conceptualization, S.M. (Sandeep Malik) and S.K.; methodology, A.B.; software, Y.Y. and L.M.; writing—original draft preparation, S.M. (Simona Moldovanu); writing—review and editing, C.I. and S.P.M.; project administration, D.B. and A.A. All authors have read and agreed to the published version of the manuscript.

Funding: This research received no external funding.

Institutional Review Board Statement: Not applicable.

Informed Consent Statement: Not applicable.

Data Availability Statement: Not applicable.

Acknowledgments: The authors thank the anonymous referees whose comments helped to improve this paper.

Conflicts of Interest: The authors declare no conflicts of interest.

References

1. Bayram, M. Optical bullets with Biswas–Milovic equation having Kerr and parabolic laws of nonlinearity. *Optik* **2022**, *270*, 170046. [CrossRef]
2. Belyaeva, T.; Serkin, V. Wave-particle duality of solitons and solitonic analog of the Ramsauer-Townsend effect. *Eur. Phys. J. D* **2012**, *66*, 1–9. [CrossRef]
3. Biswas, A. Optical soliton cooling with polynomial law of nonlinear refractive index. *J. Opt.* **2020**, *49*, 580–583. [CrossRef]
4. Gonzalez–Gaxiola, O.; Biswas, A.; Yildirim, Y.; Alshehri, H.M. Bright optical solitons with polynomial law of nonlinear refractive index by Adomian decomposition scheme. *Proc. Est. Acad. Sci.* **2022**, *71*, 213–220. [CrossRef]
5. Kudryashov, N.A.; Biswas, A.; Borodina, A.G.; Yıldırım, Y.; Alshehri, H.M. Painlevé analysis and optical solitons for a concatenated model. *Optik* **2023**, *272*, 170255. [CrossRef]

6. Kudryashov, N.A. Rational solutions of equations associated with the second Painlevé equation. *Regul. Chaotic Dyn.* **2020**, *25*, 273–280. [CrossRef]
7. Kudryashov, N.A.; Safonova, D.V. Painlevé analysis and traveling wave solutions of the sixth order differential equation with non-local nonlinearity. *Optik* **2021**, *244*, 167586. [CrossRef]
8. Kudryashov, N.A.; Safonova, D.V.; Biswas, A. Painlevé analysis and a solution to the traveling wave reduction of the Radhakrishnan-Kundu-Lakshmanan equation. *Regul. Chaotic Dyn.* **2019**, *24*, 607–614. [CrossRef]
9. Tang, L. Bifurcation analysis and multiple solitons in birefringent fibers with coupled Schrödinger-Hirota equation. *Chaos Solitons Fractals* **2022**, *161*, 112383. [CrossRef]
10. Ankiewicz, A.; Wang, Y.; Wabnitz, S.; Akhmediev, N. Extended nonlinear Schrödinger equation with higher-order odd and even terms and its rogue wave solutions. *Phys. Rev. E* **2014**, *89*, 012907. [CrossRef] [PubMed]
11. Triki, H.; Zhou, Q.; Biswas, A.; Liu, W.; Yıldırım, Y.; Alshehri, H.M.; Belic, M.R. Chirped optical solitons having polynomial law of nonlinear refractive index with self-steepening and nonlinear dispersion. *Phys. Lett. A* **2021**, *417*, 127698. [CrossRef]
12. Wang, M.Y. Optical solitons with perturbed complex Ginzburg–Landau equation in Kerr and cubic–quintic–septic nonlinearity. *Results Phys.* **2022**, *33*, 105077. [CrossRef]
13. Wazwaz, A.M.; Mehanna, M. Higher-order Sasa–Satsuma equation: Bright and dark optical solitons. *Optik* **2021**, *243*, 167421. [CrossRef]
14. Zayed, E.M.; Alngar, M.E.; Biswas, A.; Ekici, M.; Guggilla, P.; Khan, S.; Alshehri, H.M.; Belic, M.R. Optical solitons in fiber Bragg gratings with polynomial law nonlinearity and cubic–quartic dispersive reflectivity. *Opt. Spectrosc.* **2022**, *130*, 28–34. [CrossRef]
15. Zhou, Q. Influence of parameters of optical fibers on optical soliton interactions. *Chin. Phys. Lett.* **2022**, *39*, 010501. [CrossRef]
16. Akter, A.; Islam, M.J.; Atai, J. Quiescent Gap Solitons in Coupled Nonuniform Bragg Gratings with Cubic-Quintic Nonlinearity. *Appl. Sci.* **2021**, *11*, 4833. [CrossRef]
17. Islam, M.J.; Atai, J. Stability of moving Bragg solitons in a semilinear coupled system with cubic–quintic nonlinearity. *J. Mod. Opt.* **2021**, *68*, 365–373. [CrossRef]
18. Islam, M.J.; Atai, J. Dynamics of colliding counterpropagating solitons in coupled Bragg gratings with cubic-quintic nonlinearity. *J. Mod. Opt.* **2019**, *66*, 1498–1505. [CrossRef]
19. Ahmed, T.; Atai, J. Soliton-soliton dynamics in a dual-core system with separated nonlinearity and nonuniform Bragg grating. *Nonlinear Dyn.* **2019**, *97*, 1515–1523. [CrossRef]
20. Islam, M.J.; Atai, J. Soliton–soliton interactions in a grating-assisted coupler with cubic-quintic nonlinearity. *J. Mod. Opt.* **2018**, *65*, 2153–2159. [CrossRef]
21. Islam, M.J.; Atai, J. Stability of moving gap solitons in linearly coupled Bragg gratings with cubic–quintic nonlinearity. *Nonlinear Dyn.* **2018**, *91*, 2725–2733. [CrossRef]
22. Ahmed, T.; Atai, J. Bragg solitons in systems with separated nonuniform Bragg grating and nonlinearity. *Phys. Rev. E* **2017**, *96*, 032222. [CrossRef] [PubMed]
23. Sultana, J.; Islam, M.S.; Atai, J.; Islam, M.R.; Abbott, D. Near-zero dispersion flattened, low-loss porous-core waveguide design for terahertz signal transmission. *Opt. Eng.* **2017**, *56*, 076114. [CrossRef]
24. Islam, M.S.; Sultana, J.; Atai, J.; Abbott, D.; Rana, S.; Islam, M.R. Ultra low-loss hybrid core porous fiber for broadband applications. *Appl. Opt.* **2017**, *56*, 1232–1237. [CrossRef] [PubMed]
25. Jahirul Islam, M.; Atai, J. Stability of Bragg grating solitons in a semilinear dual-core system with cubic–quintic nonlinearity. *Nonlinear Dyn.* **2017**, *87*, 1693–1701. [CrossRef]
26. Chowdhury, S.S.; Atai, J. Interaction dynamics of Bragg grating solitons in a semilinear dual-core system with dispersive reflectivity. *J. Mod. Opt.* **2016**, *63*, 2238–2245. [CrossRef]
27. Cao, H.; Atai, J.; Zuo, J.; Yu, Y.; Gbadebo, A.; Xiong, B.; Hou, J.; Liang, P.; Gao, Y.; Shu, X. Simultaneous multichannel carrier-suppressed return-to-zero to non-return-to-zero format conversion using a fiber Bragg grating. *Appl. Opt.* **2015**, *54*, 6344–6350. [CrossRef]
28. Cao, H.; Shu, X.; Atai, J.; Zuo, J.; Xiong, B.; Shen, F.; Cheng, J. Fiber Bragg grating based notch filter for bit-rate-transparent NRZ to PRZ format conversion with two-degree-of-freedom optimization. *J. Opt.* **2015**, *17*, 025702. [CrossRef]
29. Cao, H.; Shu, X.; Atai, J.; Gbadebo, A.; Xiong, B.; Fan, T.; Tang, H.; Yang, W.; Yu, Y. Optimally-designed single fiber Bragg grating filter scheme for RZ-OOK/DPSK/DQPSK to NRZ-OOK/DPSK/DQPSK format conversion. *Opt. Express* **2014**, *22*, 30442–30460. [CrossRef] [PubMed]
30. Islam, M.J.; Atai, J. Stability of gap solitons in dual-core Bragg gratings with cubic-quintic nonlinearity. *Laser Phys. Lett.* **2014**, *12*, 015401. [CrossRef]
31. Cao, H.; Atai, J.; Yu, Y.; Xiong, B.; Zhou, Y.; Cai, J.; Shu, X. Carrier-suppressed return-to-zero to non-return-to-zero format conversion based on a single fiber Bragg grating with knife-shaped spectra. *Appl. Opt.* **2014**, *53*, 5649–5653. [CrossRef]
32. Dasanayaka, S.; Atai, J. Moving Bragg grating solitons in a cubic–quintic nonlinear medium with dispersive reflectivity. *Phys. Rev. E* **2013**, *88*, 022921. [CrossRef]
33. Cao, H.; Atai, J.; Shu, X.; Chen, G. Direct design of high channel-count fiber Bragg grating filters with low index modulation. *Opt. Express* **2012**, *20*, 12095–12110. [CrossRef]
34. Baratali, B.; Atai, J. Gap solitons in dual-core Bragg gratings with dispersive reflectivity. *J. Opt.* **2012**, *14*, 065202. [CrossRef]

35. Dasanayaka, S.; Atai, J. Interactions of solitons in Bragg gratings with dispersive reflectivity in a cubic-quintic medium. *Phys. Rev. E* **2011**, *84*, 026613. [CrossRef] [PubMed]
36. Dasanayaka, S.; Atai, J. Stability of Bragg grating solitons in a cubic–quintic nonlinear medium with dispersive reflectivity. *Phys. Lett. A* **2010**, *375*, 225–229. [CrossRef]
37. Carroll, S.S.; Atai, J. Collision dynamics of solitons in a multi-channel stabilized dispersion managed link. *J. Opt. A: Pure Appl. Opt.* **2009**, *11*, 085407. [CrossRef]
38. Neill, D.R.; Atai, J. Gap solitons in a hollow optical fiber in the normal dispersion regime. *Phys. Lett. A* **2007**, *367*, 73–82. [CrossRef]
39. Atai, J.; Malomed, B.A.; Merhasin, I.M. Stability and collisions of gap solitons in a model of a hollow optical fiber. *Opt. Commun.* **2006**, *265*, 342–348. [CrossRef]
40. Neill, D.R.; Atai, J. Collision dynamics of gap solitons in Kerr media. *Phys. Lett. A* **2006**, *353*, 416–421. [CrossRef]
41. Atai, J.; Malomed, B.A. Gap solitons in Bragg gratings with dispersive reflectivity. *Phys. Lett. A* **2005**, *342*, 404–412. [CrossRef]
42. Atai, J.; Malomed, B.A. Stability and interactions of solitons in asymmetric dual-core optical waveguides. *Opt. Commun.* **2003**, *221*, 55–62. [CrossRef]
43. Atai, J.; Malomed, B.A. Spatial solitons in a medium composed of self-focusing and self-defocusing layers. *Phys. Lett. A* **2002**, *298*, 140–148. [CrossRef]
44. Nistazakis, H.; Frantzeskakis, D.; Atai, J.; Malomed, B.; Efremidis, N.; Hizanidis, K. Multichannel pulse dynamics in a stabilized Ginzburg-Landau system. *Phys. Rev. E* **2002**, *65*, 036605. [CrossRef] [PubMed]
45. Atai, J.; Malomed, B.A. Solitary waves in systems with separated Bragg grating and nonlinearity. *Phys. Rev. E* **2001**, *64*, 066617. [CrossRef]
46. Atai, J.; Malomed, B.A. Families of Bragg-grating solitons in a cubic–quintic medium. *Phys. Lett. A* **2001**, *284*, 247–252. [CrossRef]
47. Arnous, A.H.; Zhou, Q.; Biswas, A.; Guggilla, P.; Khan, S.; Yıldırım, Y.; Alshomrani, A.S.; Alshehri, H.M. Optical solitons in fiber Bragg gratings with cubic–quartic dispersive reflectivity by enhanced Kudryashov's approach. *Phys. Lett. A* **2022**, *422*, 127797. [CrossRef]
48. Tanwar, D.V.; Kumar, M.; Tiwari, A.K. Lie symmetries, invariant solutions and phenomena dynamics of Boiti–Leon–Pempinelli system. *Phys. Scr.* **2022**, *97*, 075209. [CrossRef]
49. Tanwar, D.V. Lie symmetry reductions and generalized exact solutions of Date–Jimbo–Kashiwara–Miwa equation. *Chaos Solitons Fractals* **2022**, *162*, 112414. [CrossRef]
50. Tanwar, D.V.; Kumar, M. On Lie symmetries and invariant solutions of Broer–Kaup–Kupershmidt equation in shallow water of uniform depth. *J. Ocean. Eng. Sci.* 2022, *in press*. [CrossRef]
51. Tanwar, D.V. Optimal system, symmetry reductions and group-invariant solutions of (2+ 1)-dimensional ZK-BBM equation. *Phys. Scr.* **2021**, *96*, 065215. [CrossRef]
52. Tanwar, D.V.; Wazwaz, A.M. Lie symmetries and exact solutions of KdV–Burgers equation with dissipation in dusty plasma. *Qual. Theory Dyn. Syst.* **2022**, *21*, 164. [CrossRef]
53. Bluman, G.W.; Cheviakov, A.F.; Anco, S.C. *Applications of Symmetry Methods to Partial Differential Equations*; Springer: Berlin/Heidelberg, Germany, 2010; Volume 168.
54. Arrigo, D.J. *Symmetry Analysis of Differential Equations: An Introduction*; John Wiley & Sons: Hoboken, NJ, USA, 2015.
55. Cherniha, R.; Serov, M.; Pliukhin, O. *Nonlinear Reaction-Diffusion-Convection Equations: Lie and Conditional Symmetry, Exact Solutions and Their Applications*; CRC Press: Boca Raton, FL, USA, 2017.
56. Hydon, P.E. *Symmetry Methods for Differential Equations: A Beginner's Guide*; Number 22; Cambridge University Press: Cambridge, UK, 2000.
57. Bluman, G.; Anco, S. *Symmetry and Integration Methods for Differential Equations*; Springer Science & Business Media: Berlin/Heidelberg, Germany, 2008; Volume 154.
58. Habiba, U.; Salam, M.A.; Hossain, M.B.; Datta, M. Solitary wave solutions of Chafee-Infante equation and (2 + 1)-dimensional breaking soliton equation by the improved Kudryashov method. *Glob. J. Sci. Front. Res.* **2019**, *19*, 1–9. [CrossRef]
59. Malik, S.; Kumar, S. Pure-cubic optical soliton perturbation with full nonlinearity by a new generalized approach. *Optik* **2022**, *258*, 168865. [CrossRef]
60. Wazwaz, A.M. The extended tanh method for new solitons solutions for many forms of the fifth-order KdV equations. *Appl. Math. Comput.* **2007**, *184*, 1002–1014. [CrossRef]